A peer-reviewed version of this preprint was published in PeerJ on 2 September 2014.

View the peer-reviewed version (peerj.com/articles/551), which is the preferred citable publication unless you specifically need to cite this preprint.

Silva PJ. 2014. With or without light: comparing the reaction mechanism of dark-operative protochlorophyllide oxidoreductase with the energetic requirements of the light-dependent protochlorophyllide oxidoreductase. PeerJ 2:e551 https://doi.org/10.7717/peerj.551

With or without light: comparing the reaction mechanism of dark-operative protochlorophyllide oxidoreductase with the energetic requirements of the light-dependent protochlorophyllide oxidoreductase

Pedro J Silva

The addition of two electrons and two protons to the C_{17}=C_{18} bond in protochlorophyllide is catalyzed by a light-dependent enzyme relying on NADPH as electron donor, and by a light-independent enzyme bearing a $(Cys)_3$Asp-ligated [4Fe-4S] cluster which is reduced by cytoplasmic electron donors in an ATP-dependent manner and then functions as electron donor to protochlorophyllide. The precise sequence of events occurring at the C_{17}=C_{18} bond has not, however, been determined experimentally in the dark-operating enzyme. In this paper, we present the computational investigation of the reaction mechanism of this enzyme at the B3LYP/6-311+G(d,p)// B3LYP/6-31G(d) level of theory. The reaction mechanism begins with single-electron reduction of the substrate by the $(Cys)_3$Asp-ligated [4Fe-4S], yielding a negatively-charged intermediate. Depending on the rate of Fe-S cluster re-reduction, the reaction either proceeds through double protonation of the single-electron-reduced substrate, or by alternating proton/electron transfer The computed reaction barriers suggest that Fe-S cluster re-reduction should be the rate-limiting stage of the process. Additional comparisons of the energetic features of the intermediates with those of common biochemical redox intermediates suggest a surprisingly simple explanation for the mechanistic differences between the dark-catalyzed and light-dependent enzyme reaction mechanisms.

PeerJ PrePrints | http://dx.doi.org/10.7287/peerj.preprints.302v1 | CC-BY 3.0 Open Access | received: 25 Mar 2014, published: 25 Mar 2014

Pedro J. Silva[*]

REQUIMTE, Fac. de Ciências da Saúde, Universidade Fernando Pessoa, Rua Carlos da Maia, 296,

4200-150 Porto-Portugal

*pedros@ufp.edu.pt

PeerJ PrePrints | http://dx.doi.org/10.7287/peerj.preprints.302v1 | CC-BY 3.0 Open Access | received: 25 Mar 2014, published: 25 Mar 2014

Introduction

All life on Earth depends on the availability of reduced forms of carbon. As the reduction of simple carbon-containing molecules like CO_2 is a strongly endergonic process, additional sources of energy are needed to overcome this high thermodynamic hurdle. Although several organisms (collectively known as lithoautotrophs) are able to obtain that energy from the conversion of inorganic substances, the overwhelming majority of carbon reduction is performed by photosynthetic organisms, which obtain the necessary energy by capturing photons from visible light. These photons are used to excite chromophores, which then become highly efficient reducing species, ultimately providing both the low-potential electrons needed to reduce carbon and the ATP used by cells as energy-transfer molecule. The most abundant photosynthetic pigments, chlorophylls, are obtained from the tetrapyrrole protoporphyrin IX through a series of reactions that includes Mg^{2+} complexation, methylation by an S-adenosylmethionine-dependent methyltransferase and six-electron oxidation, yielding an highly-unsaturated molecule, protochlorophyllide (PChlide), which absorbs mainly in the low-energy region of the spectrum and is therefore unable to drive the necessary charge separation in the photosynthetic reaction centers(Masuda & Fujita, 2008). Two different enzymes are able to increase the saturation of the PChlide ring and generate chlorophyllide (Chlide), a pigment that absorbs light in higher-energy regions of the spectrum: angiosperms contain an oxygen-insensitive light-dependent protochlorophyllide oxidoreductase(Masuda & Takamiya, 2004), whereas gimnosperms, algae and cyanobacteria possess an oxygen sensitive, dark-operating, protochlorophyllide oxidoreductase(Fujita & Bauer, 2003) evolutionarily related to nitrogenase.

The reaction mechanism of the light-dependent protochlorophyllide oxidoreductase has been extensively studied through experimental(Heyes & Hunter, 2004; Heyes et al., 2009, 2011; Sytina et al., 2012) and computational(Heyes et al., 2009; Silva & Ramos, 2011) methods. In contrast, relatively little is known about the precise sequence of events taking place in the dark-operative protochlorophyllide oxidoreductase (dPCHOR). The enzyme contains two components: a homodimeric L-protein which

PeerJ PrePrints | http://dx.doi.org/10.7287/peerj.preprints.302v1 | CC-BY 3.0 Open Access | received: 25 Mar 2014, published: 25 Mar 2014

performs ATP-dependent electron transfer reminiscent of that observed in nitrogenase Fe protein(Fujita & Bauer, 2000; Sarma et al., 2008), and a heterotetrameric component bearing the active site and a $(Cys)_3Asp$-ligated [4Fe-4S] cluster which accepts electrons from the L-protein and functions as the electron donor to the protochlorophyllide substrate(Bröcker et al., 2010; Muraki et al., 2010). The peculiar ligation of the electron-transferring [4Fe-4S] cluster has been shown by site-directed mutagenesis to be crucial to the enzyme activity(Muraki et al., 2010), probably due to the lowering of its reduction potential below that of other [4Fe-4S] clusters.(Kondo et al., 2011; Takano et al., 2011) The crystallographic structure of dPCHOR(Bröcker et al., 2010; Muraki et al., 2010) shows that the substrate binding site, while mostly lined by hydrophobic residues, contains a single conserved aspartate residue (Asp274) which is thought to be a proton-donor for the reaction. Two protons and two electrons are required (Fig. 1), which necessarily entails two separate reduction events (as the [4Fe-4S] cluster is a one-electron donor) and the presence of a second proton-donor. Asp274 is unlikely to act as the donor of the second proton, as it cannot be reprotonated due to the absence of pathways linking it to the solvent. The propionic acid side-chain present on the substrate C_{17} was therefore proposed as the second proton donor(Muraki et al., 2010). The intricacies of proton and electron transfer from dPChOR to its protochlorophyllide substrate have, however, remained unaddressed by experimental methods. In this report, we describe this reaction mechanism with the help of density-functional methods. The results allow the description of the sequence of the reduction/protonation events and also identify the factors governing the stereochemical outcome of this enzyme-catalyzed reaction. Comparisons of the energetic features of the intermediates with those of common biochemical redox intermediates suggest a simple explanation for the differences observed in the dark-catalyzed and light-dependent enzyme reactions.

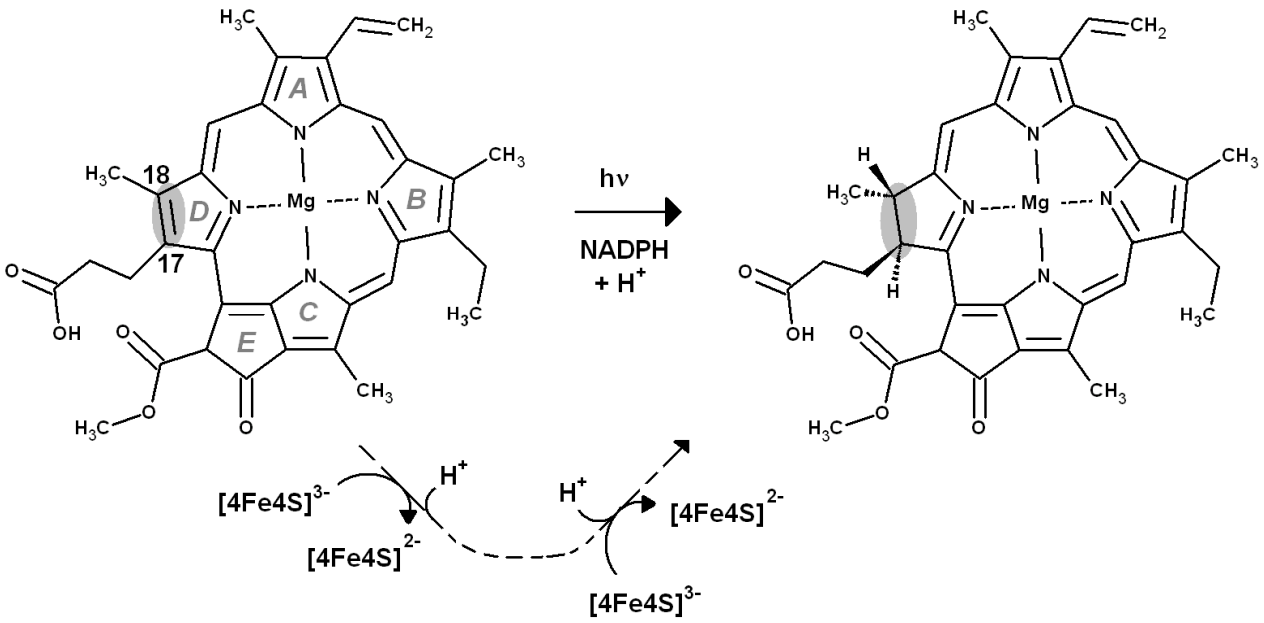

Figure 1: Comparison of the overall reaction mechanisms of light-dependent (central pathway) and dark-operative (bottom pathway) protochlorophyllide oxidoreductases. The rings have been labeled according to the IUPAC nomenclature.(Moss, 1987)

Computational methods

Coordinates of the active site were taken from the X-ray structure (3AEK) determined by Muraki et al.(Muraki et al., 2010). Since the substrate binding cavity is almost completely lined with hydrophobic residues (which are generally uninteresting from a reactional point of view) the computational model of the active site could be thoroughly pruned, to achieve a cost-effective computational model: computations with a very simplified substrate mimic (4-methyl-2,5-dimethylidene-2,5-dihydro-1H-pyrrol-3-yl)acetic acid, the proton-donating Asp274, and the second-shell aminoacids Arg48 (which is located close to the proton-donating Asp274) and Gly409-Leu410 backbone (which may establish a single hydrogen bond to the propionic acid present on the substrate) showed that neglect of the second-shell amino acids affects proton-transfer energies by less than 2 kcal.mol^{-1}. The reaction mechanism was therefore studied using the complete natural substrate, the water molecule bound to its Mg atom, and the

only amino acid sidechain (Asp 274) able to interact with the substrate through hydrogen-bonds and/or proton donation. To prevent unrealistic movements of the simplified computational model, the protochlorophyllide Mg atom and the Asp274 C_α and C_β carbon atoms were constrained to their crystallographic positions. Geometry optimizations were performed with the Firefly(Granovsky, 2013) quantum chemistry package, which is partially based on the GAMESS (US)(Schmidt et al., 1993) source code, at the B3LYP(Lee, Yang, & Parr, 1988; Becke, 1993; Hertwig & Koch, 1995) level with the 6-31G(d) basis set, using autogenerated delocalized coordinates(Baker, Kessi, & Delley, 1996). Zero-point and thermal effects on the enthalpies/free energies at 298 K were computed at the optimized geometries using a scaling factor of 0.9804. Single-point energies were computed with the triple-zeta 6-311G(d,p) basis set, augmented with a set of diffuse functions on the oxygen, henceforth called 6-311G(+)(d,p).

The $Asp(Cys)_3$-ligated Fe-S cluster was optimized separately in the reduced and oxidized forms, using the SBKJC effective core potential and associate basis set for Fe and 6-31G(d) for the other elements. The C_α and C_β carbon atoms of the coordinating amino acids were constrained to their crystallographic positions to prevent unrealistic movements and to capture the subtle influence of the conformation of the cysteinyl sidechains on the redox potential of the Fe-S cluster(Niu & Ichiye, 2009). Appropriate broken-symmetry initial guesses of the Fe-S cluster density were generated using a combination of the protocols of Szilagyi(Szilagyi & Winslow, 2006) and Greco(Greco et al., 2010). Single-point energies of the optimized geometries of the Fe-S cluster were computed using the all-electron s6-31G* basis set(Swart et al., 2010) for Fe and 6-311G(2d,p) for all other elements. Intra- and inter-molecular dispersion effects were computed with the DFT-D3 formalism developed by Grimme *et al.*(Grimme et al., 2010). The activation energy of the one-electron transfer between the reduced Fe-S cluster and the substrate was estimated by applying Marcus theory for electron transfer, as suggested by Blomberg and Siegbahn(Blomberg & Siegbahn, 2003). Reorganization energies for the Fe-S cluster and substrate in each oxidation state were computed using the reactant geometry for the product state (e.g. the oxidized state energy is computed at the reduced Fe-S cluster geometry, etc.) and vice-versa. Activation energies

were then computed by building appropriate Marcus parabolas using these reorganization energies, as shown in Scheme 1.

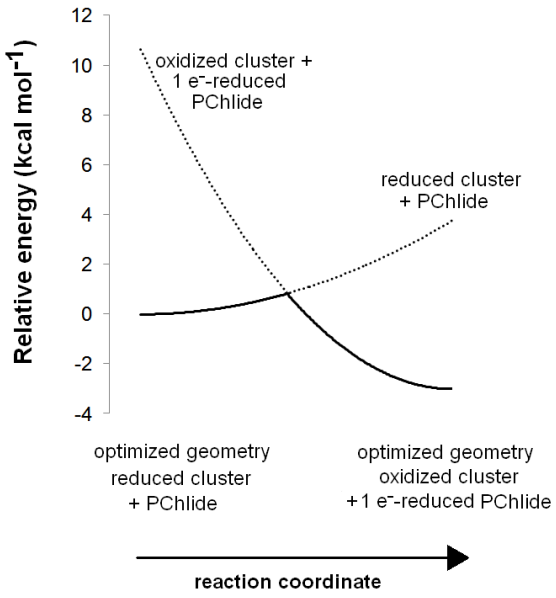

Scheme 1

All energy values described in the text include solvation effects (ε=10) computed using the Polarizable Continuum Model(Tomasi & Persico, 1994; Mennucci & Tomasi, 1997; Cossi et al., 1998) implemented in Firefly. ε=10 was chosen instead of the more common ε=4 to model some of the stabilization of the ionic forms of Asp274 and propionic acid residues provided in the enzyme by hydrogen bonding with the Gly409-Leu410 backbone amide. Energies computed at other dielectric constants are shown in Table 1.Energies of reactions involving addition of *n* non-modeled solvent protons were computed as :

$$\Delta G = \Delta G_{\text{solvated products}} - \Delta G_{\text{solvated reactants}} - n\,\Delta G_{\text{solvated H+}}$$

For the solvation free energy of H^+, $\Delta G_{solv,\ H+}$, we used the value of -265.9 kcal mol^{-1}, obtained by converting the experimental value of -263.98 kcal mol-1 (Tissandier *et al.*(Tissandier et al., 1998)) to the appropriate thermodynamic standard state conventions as recommended by Kelly *et al.*(Kelly, Cramer, & Truhlar, 2006). To enable direct comparison of energies with a different number of non-modeled solvent protons, these ΔG values were then converted to effective ΔG at pH=7.0 :

$$\Delta G_{eff} = \Delta G - RT \ln [H^+]^n .$$

Energy differences between *n*-electron containing species and the corresponding *n+1*-electron-containing analogues were converted to reduction potentials (ΔE) through

$$\Delta G = -n F \Delta E$$

, where *n* is the number of electrons added to the species and F is the Faraday constant (96485 $C.mol^{-1}$).

Results and discussion

In the crystal structure, Asp274 lies in the proper position to yield an intermediate with the correct stereochemistry only if it acts as proton donor to C_{17}. Therefore, we began our investigations assuming that Asp274 protonates C_{17} and the propionic acid sidechain protonates C_{18}. We also computed the reaction energetic for the proton transfers leading to the products with the wrong stereochemistries on C_{17} and C_{18}.

Proton-transfer events

The experimentally-obtained enzyme activity of dPChOR(Muraki et al., 2010) (50 nmol·min^{-1}·mg^{-1}) sets an upper limit of 19.3 kcal·mol^{-1} for the rate-determining step of its reaction mechanism, using the well-known Eyring equation, $k_{cat} = \frac{k_B T}{h} e^{-\frac{\Delta G^{\ddagger}}{RT}}$, where k_{cat} is the measured rate-constant, k_B is the Boltzmann constant, h is the Planck constant and $\Delta G^{\ddagger}$ is the activation free energy. The initial generation of a reaction intermediate from proton-transfer from Asp274 to C_{17} can therefore be ruled out, as its energy lies 31.4 kcal·mol^{-1} above the reactant state (Table 1). In contrast, the computed barrier for the proton transfer from the propionic sidechain to C_{18} (24.7 kcal·mol^{-1}) agrees reasonably well with the experimental value. The difference in computed stabilities between the C_{17}- and C-$_{18}$-protonated isomers is more pronounced in the gas phase, which shows that the most important factor favoring the C_{18}- over the C_{17}- isomer is of an electrostatic nature. Indeed, although both systems contain a positive charge in the substrate aromatic ring and a negative charge on a carboxylate group, the distance between these charges is much larger in the C_{17}-isomer/Asp274 carboxylate system.

Table 1: Relative enthalpies (in kcal mol^{-1}) of all intermediates and transition states in the reaction mechanism of light-independent protochlorophyllide oxidoreductase, computed at the B3LYP/6-311+G(d,p)// B3LYP/6-31G(d) level of theory. ZPVE and solvation effects at several dielectric constants (ε) are included. *) Wrong stereochemistry on the protochlorophyllide C_{17} or C_{18} atoms.

Added electrons	Proton on…	Proton on…	ε =4	ε =10	ε =20	ε =78.36
0	Asp274	propionate	0.0	0.0	0.0	0.0
0	Asp274	Propionate … C18	24.0	24.7	25.0	25.2
0	Asp274	C18	19.7	19.8	19.9	19.9
0	Asp274 … C17	propionate	31.3	31.4	31.5	31.6
0	C17	propionate	26.3	25.3	25.0	24.7
1	Asp274	propionate	-62.2	-67.4	-69.3	-70.7
1	Asp274… C17	propionate	-49.1	-53.8	-55.5	-56.8
1	C17	propionate	-64.5	-70.5	-72.6	-74.2
1	Asp274	Propionate … C18	-53.3	-58.3	-60.0	-61.3
1	Asp274	C18	-68.5	-73.9	-75.9	-77.3
1	Asp274… C17	C18	-50.2	-55.1	-56.7	-58.0
1	C17	Propionate … C18	-54.2	-59.7	-61.6	-63.0
1	C17	C18	-68.4	-75.6	-78.1	-79.9
1	C18*	propionate	-53.9	-59.6	-61.6	-63.1
1	Asp274	C17*	-51.9	-58.4	-60.7	-62.5
2	Asp274	propionate	-101.5	-121.2	-128.1	-133.4
2	Asp274… C17	propionate	-94.6	-112.7	-119.0	-123.8
2	C17	propionate	-123.3	-142.1	-148.6	-153.5
2	Asp274	Propionate … C18	-98.2	-116.4	-122.8	-127.6
2	Asp274	C18	-119.2	-138.7	-145.5	-150.7
2	C17	Propionate … C18	-126.8	-145.3	-151.7	-156.6
2	Asp274… C17	C18	-124.9	-143.7	-150.2	-155.1
2	C17	C18	-160.1	-179.1	-185.6	-190.5
2	C18*	propionate	-112.5	-130.5	-136.7	-141.4
2	Asp274	C17*	-113.4	-132.9	-139.6	-144.8

PeerJ PrePrints | http://dx.doi.org/10.7287/peerj.preprints.302v1 | CC-BY 3.0 Open Access | received: 25 Mar 2014, published: 25 Mar 2014

In the one-electron-reduced state, the excess spin is, as expected, strongly delocalized across the porphyrin π–system (≈0.1 spin each on rings B and D, ≈0.25 on ring A, ≈0.30 on the C/E rings, and the remaining spin on the methylene bridges). In this state, the proton uptake becomes much more favorable than before (by >15 kcal·mol^{-1}, irrespective of the protonation site), due to the formation of a neutral protochlorophyllide/negative carboxylate intermediate, rather than the charge-separated pair observed in the non-reduced state. Proton-transfer to C_{18} is predicted to occur with a very small barrier of 9.2 kcal·mol^{-1}, whereas the proton-transfer from Asp274 to C_{17} has a larger barrier of 13.6 kcal.mol^{-1}. This difference in barriers seems to be correlated to the proton/protochlorophyllide distance observed in the transition state (1.46 Å for the Asp274-C_{17} transfer vs. 1.31 Å for the carboxylate sidechain-C_{18} transfer). The transfer of an additional proton to the one-electron-reduced/singly-protonated substrated may then occur with moderate barriers. The transfer from the propionic side chain to C_{18} is again faster than that of Asp274 to C17 (10.8 kcal·mol^{-1}, vs. 18.9 kcal·mol^{-1}). The total barrier for the two consecutive proton-transfer events at the one-electron-reduced is fully consistent with the experimental value, regardless of the precise sequence of these events (13.6 kcal·mol^{-1} for Asp274-C_{17} transfer followed by propionic sidechain-C_{18} transfer; 18.9 kcal mol^{-1} for the sequence initiated with transfer to C_{18}).

In the two-electron-reduced state, the barrier for the Asp_{274}-C_{17} proton transfer (8.5 kcal·mol^{-1}) is almost as low as the barrier for the proton transfer from the propionic sidechain to the C_{18} atom (4.8 kcal·mol^{-1}). Transfer of the second proton to the ring occurs without an enthalpic barrier in both cases, yielding the chlorophyllide product with the deprotonated Asp274 and propionate sidechain.

Analysis of alternative protonation events was also performed, to ascertain the reasons behind the observed stereochemical outcome. These computations showed that proton transfer from the propionic acid sidechain to C_{17} (yielding the wrong configuration in this carbon atom) is less favorable than any of the stereochemically correct proton transfers (Asp274 to C_{17} and propionic acid to C_{18}), even in our simplified models which do not include the full steric constraints imposed by the hydrophobic

PeerJ PrePrints | http://dx.doi.org/10.7287/peerj.preprints.302v1 | CC-BY 3.0 Open Access | received: 25 Mar 2014, published: 25 Mar 2014

aminoacids lining the active site. The difference in electronic energies amounts to 11 kcal·mol^{-1} in the one-electron-reduced state, and to 8.5 kcal mol^{-1} at the two-electron-reduced state. This intermediate contains (especially at the one-electron-reduced state) an unfavorable steric interaction, as the wrong configuration at C_{17} pushes the propionate sidechain towards Asp274 (Figure 2). Protonation of C_{18} by Asp274, which generates the wrong configuration on C_{18}, is also less favorable by 16 kcal mol^{-1} at the one-electron-reduced state, and by 9.5 kcal mol^{-1} at the two-electron-reduced-state. This destabilization occurs in spite of the lack of sterical clashes because no favorable stabilizing interactions of the carboxylate in Asp274 with the Mg^{2+}-coordinating water are possible in this isomer, in contrast to the correct isomer that arises when the carboxylate forms on the propionic acid sidechain.

PeerJ PrePrints | http://dx.doi.org/10.7287/peerj.preprints.302v1 | CC-BY 3.0 Open Access | received: 25 Mar 2014, published: 25 Mar 2014

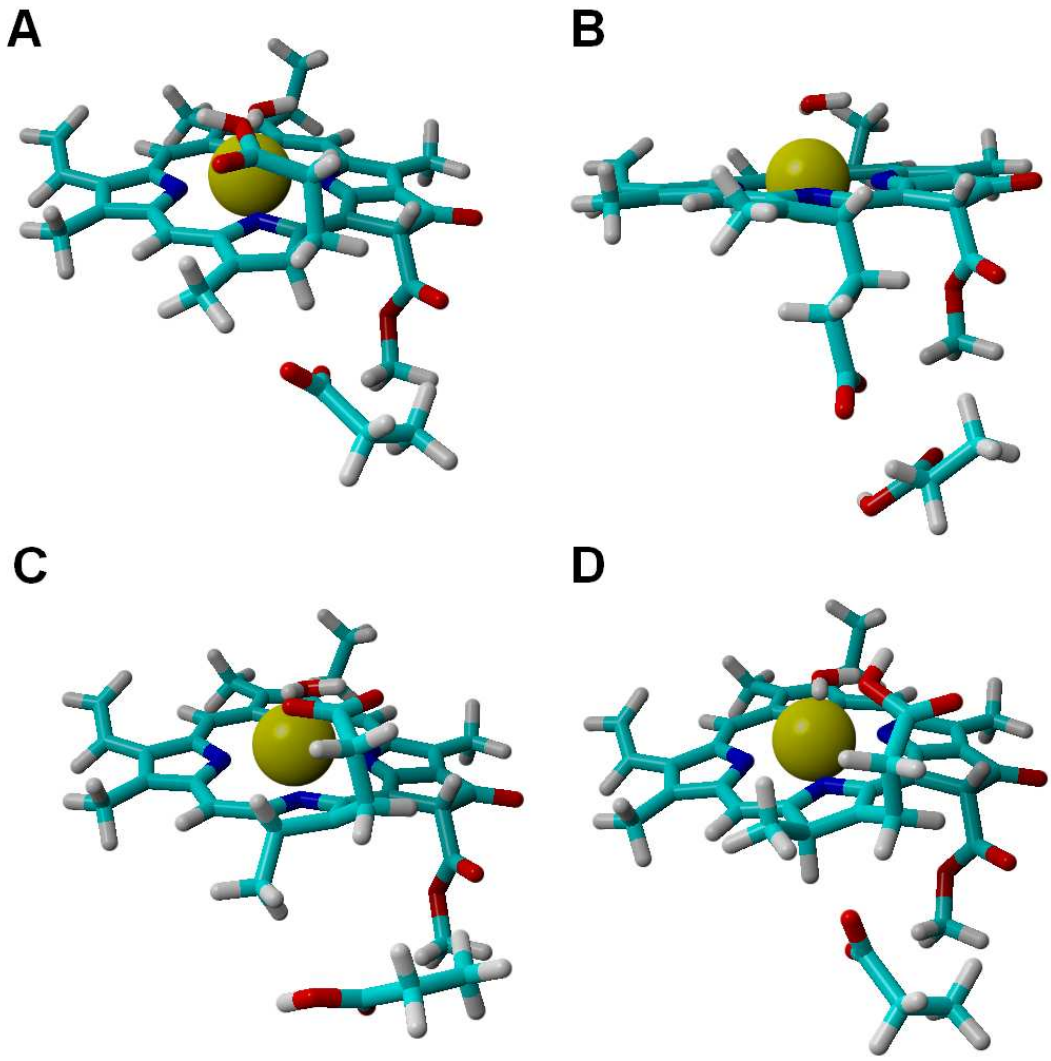

Figure 2: Comparison of the structures bearing a singly-protonated C_{17}=C_{18} bond at the one-electron-reduced state. A) Bond protonated on C_{17} by Asp274 (correct stereochemistry); B) Bond protonated on C_{17} by the propionic acid sidechain (wrong stereochemistry); C) Bond protonated on C_{18} by the propionic acid sidechain (correct stereochemistry); D) Bond protonated on C_{18} by Asp274 (wrong stereochemistry);

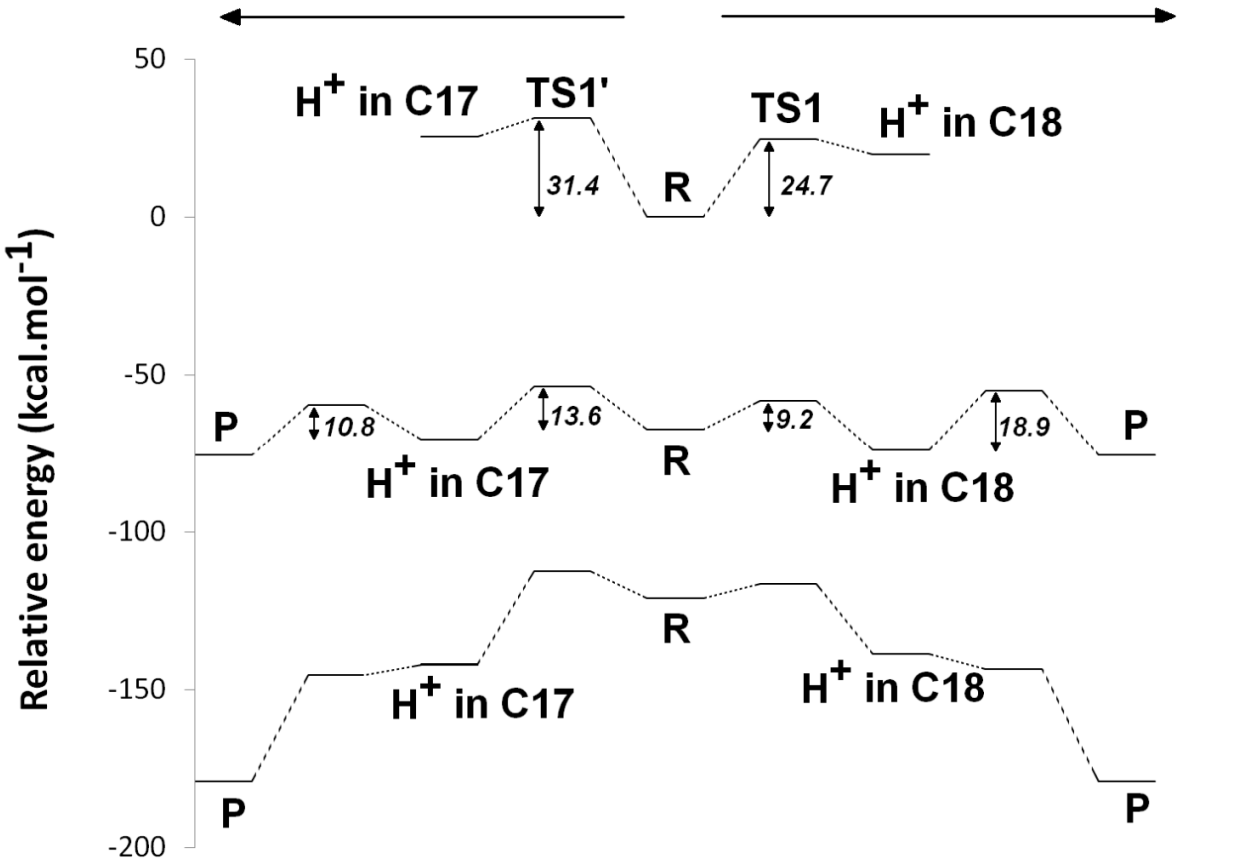

Figure 3: Potential energy surfaces of proton and electron transfer events in light-independent PChOR, computed at the B3LYP/6-311G(+)(d,p)// B3LYP/6-31G(d) level of theory with ε=10. The upper trace represents the potential energy surface (PES) with no added electrons; middle trace: PES at the one-electron-reduced state; lower trace: PES at the two-electron-reduced state. The energetic distance between the potential energy surfaces computed at different reduction states may be converted to redox potentials, as described in the methods section and discussed in the text.

Electron-transfer events

The ease of reduction of each intermediate may be easily computed by taking the difference of energies between any *n*-electron containing species and the corresponding *n*+1-electron-containing analogues. It can easily be seen (Table 2, last column), that one-electron reduction of the reaction intermediates depends strongly on the charge present on the PChlide ring: species with negative or neutral protochlorophyllide rings have an absolute redox potential between 2.3 and 3.2 V, whereas intermediates bearing one or more positive charges have much more favorable absolute redox potentials between 4.0 V and 4.5 V. In dark-operating PChOR, the electron-donating species is an unusual $(Cys)_3$Asp-ligated [4Fe-4S] cluster, which has been assigned a redox potential of 3.1 V in previous computations(Takano et al., 2011). Since those computations were performed without geometrical constrains and with very truncated cysteine models (SCH_3) which do not allow the evaluation of the influence of the sidechain geometry on the electronic properties of the clusters(Niu & Ichiye, 2009), we performed additional optimizations of the Fe-S cluster using ethanethiol as model for the cysteine sidechains and appropriate constraining of their carbon atoms to their crystallographic positions. The absolute redox potential of the electron-donating $(Cys)_3$Asp-ligated [4Fe-4S] cluster in PChOR is thus computed to be 2.80 V, which implies that, in the absence of significant interactions between cluster and substrate, all electron-uptake events by protochlorophyllide (except those from the 1-electron-reduced substrate to the 2-electron reduced state and from the 1-electron-reduced, C_{18}-protonated substrate to the corresponding 2-electron reduced state) should be thermodynamically favorable, as electrons spontaneously move from the species with lower redox potentials to the ones with higher potentials. Additional single-point computations were then performed in models including the separately-optimized Fe-S clusters and reaction intermediates at their crystallographic positions to ascertain the mutual influence of the Fe-S electronic distribution on the redox potential of the reaction intermediates, and vice-versa (Table 2). Irrespective of the redox state of the Fe-S cluster, the reaction intermediates

PeerJ PrePrints | http://dx.doi.org/10.7287/peerj.preprints.302v1 | CC-BY 3.0 Open Access | received: 25 Mar 2014, published: 25 Mar 2014

become harder to reduce by 0.1-0.15 V in the original, non-reduced, state, and by 0.25-0.4 V in the one-electron-reduced state. The electric dipoles of the reaction intermediates in turn lower the Fe-S cluster redox potential (i.e. facilitate its oxidation) by similar modest amounts (0.1-0.15 V), irrespective of the number of extra electrons present on the substrate. These data also show that the oxidation state of the Fe-S cluster barely affects the energetics of the substrate protonation reactions and, consequently, should also barely affect their activation barriers.

The electronic energies of the combined Fe-S cluster/active site systems show that electron-transfer from the reduced Fe-S cluster to the protochlorophylide intermediates is thermodynamically favored in almost all cases (Table 2), except for the reduction of the one-electron-reduced/C_{18}-protonated species , which is unfavorable by a few kcal.mol^{-1}. For this thermodynamically disfavored reduction step no activation energy could be computed through the Marcus formalism as the parabolas do not touch (see Supporting Information), but comparisons with the reorganization energies at lower dielectric constants (at which this transfer becomes spontaneous) suggest that the barrier should not be too different from the others. For the spontaneous steps the electronic reorganization energies of the combined Fe-S cluster/active site systems are quite low, yielding activation energies below 4 kcal.mol^{-1}, which entails that) reduction will generally be much faster than the protonation events, which were shown above to have activation energies in excess of 10 kcal.mol^{-1}. Electron transfer from the reduced Fe-S cluster should therefore precede each protonation event, though only if the rate of re-reduction of the Fe-S cluster by the ATP-dependent L-protein(Kondo et al., 2011) does not become limiting. Two possible pathways emerge from this analysis, both arising from an initial one-electron transfer to the protochlorophyllide. In one of them (Figure 4A), re-reduction of the Fe-S cluster is slower that any of the proton-transfer events at the one-electron reduced state, which leads to the generation of a doubly protonated intermediated, preferably through the initial protonation at C_{17}, which has a lower overall barrier (13.6 kcal.mol^{-1}) than the double-protonation starting with the C_{18} atom (18.9 kcal.mol^{-1}, as discussed earlier). After both protonations and cluster re-reduction occurs, electron transfer is both very spontaneous and quite fast. In the second alternative (Figure 4B) re-reduction of the Fe-S cluster is not

PeerJ PrePrints | http://dx.doi.org/10.7287/peerj.preprints.302v1 | CC-BY 3.0 Open Access | received: 25 Mar 2014, published: 25 Mar 2014

rate-limiting and the second electron transfer to the substrate may occur immediately after the first protonation: in this instance, the reaction will likely proceed through protonation of C_{18} by the propionic acid substituent of the protochlorophyllide D-ring, followed by electron transfer and barrier-less transfer of the second proton from Asp274 to C_{17}. This pathway affords a barrier below 10 kcal mol^{-1} and reaction rates far in excess of those observed experimentally, suggesting that Fe-S cluster re-reduction should indeed be the rate-limiting stage of the process.

PeerJ PrePrints | http://dx.doi.org/10.7287/peerj.preprints.302v1 | CC-BY 3.0 Open Access | received: 25 Mar 2014, published: 25 Mar 2014

Table 2: Relative enthalpies (in kcal mol^{-1}) of intermediates in the reaction mechanism of light-independent protochlorophyllide oxidoreductase in the presence of (independently optimized) $(Cys)_3Asp$-ligated [4Fe-4S] cluster.computed at the B3LYP/6-311(+)G(d,p) – s6-31G* (Fe)– 6-311G(2d,p) (non-Fe atoms in the Fe-S cluster)// B3LYP/6-31G(d) level of theory. Solvation effects at ε=10 are included.

Added electrons	H^+ in	H^+ in	Relative energy (with reduced cluster)	Relative energy (with oxidized cluster)	Fe-S redox potential (V)	substrate redox potential (with reduced cluster) (V)	substrate redox potential (with oxidized cluster) (V)	substrate redox potential (in the absence of cluster) (V)
0	Asp274	propionate	0.00	0.00	2.70	2.78	2.81	2.92
0	Asp274	C18	20.34	19.98	2.69	3.90	3.91	4.06
0	C17	propionate	25.36	25.25	2.70	3.95	3.97	4.15
1	Asp274	propionate	-64.05	-64.70	2.67	n.d	n.d	2.33
1	Asp274	C18	-69.64	-70.17	2.68	2.47	2.49	2.81
1	C17	propionate	-65.73	-66.24	2.68	2.83	2.85	3.11
1	C17	C18	-72.20	-72.14	2.70	4.22	4.25	4.49
2	Asp274	C18	-126.58	-127.57	2.66	n.a.	n.a.	n.a.
2	C17	propionate	-131.10	-132.04	2.66	n.a.	n.a.	n.a.
2	C17	C18	-169.60	-170.10	2.68	n.a.	n.a.	n.a.

PeerJ PrePrints | http://dx.doi.org/10.7287/peerj.preprints.302v1 | CC-BY 3.0 Open Access | received: 25 Mar 2014, published: 25 Mar 2014

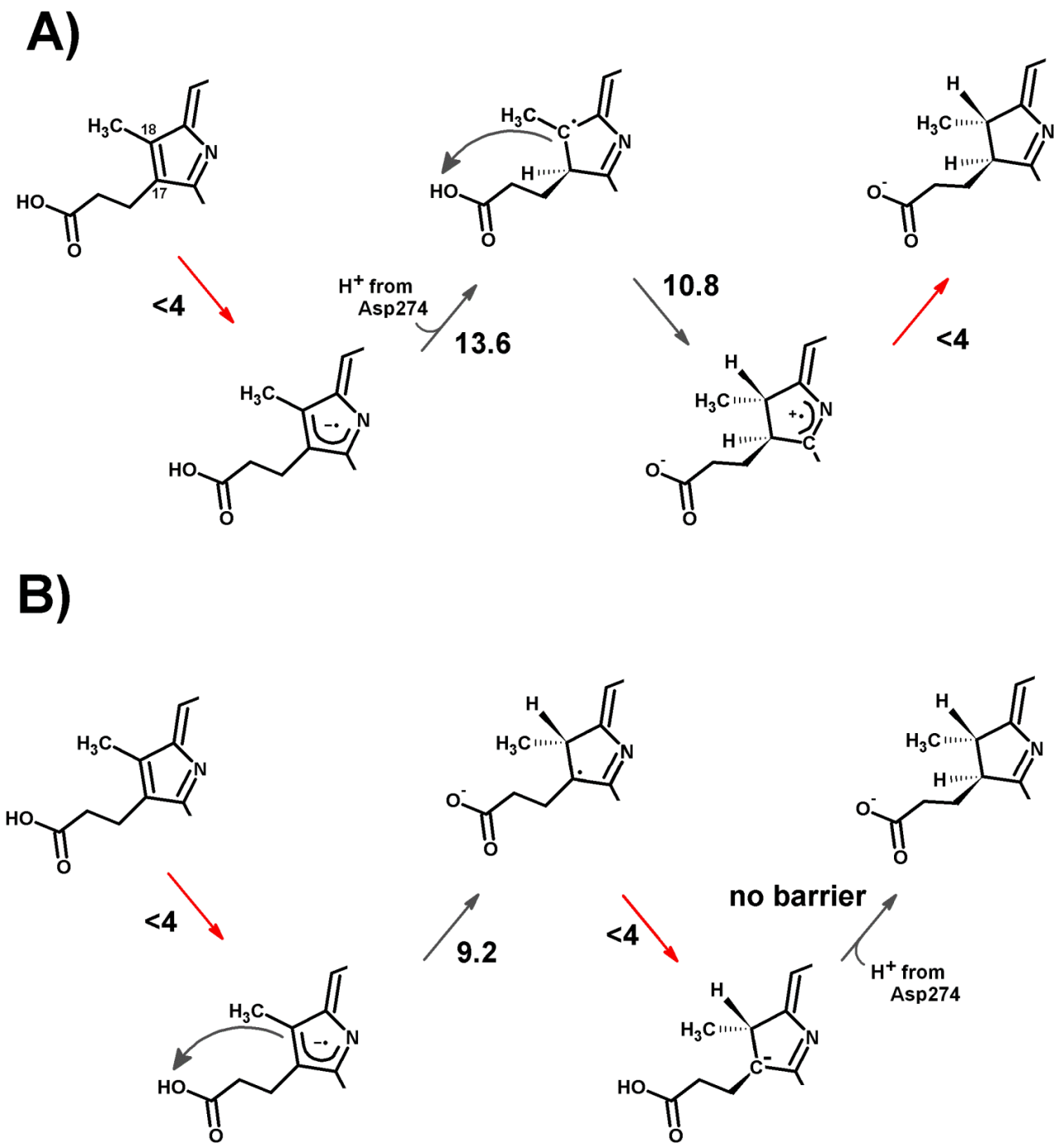

Figure 4: Schematic representation of the most-favored computed reaction mechanisms. A) Slow Fe-S cluster re-reduction . B) Fast re-redcution of the Fe-S cluster. Red arrows show the electron-transfer steps. Relevant activation energies (in kcal.mol^{-1}) are shown for each reaction step. For simplicity, only the D ring of protochlorophyllide is represented.

Energetic comparison to the light-dependent reaction

PeerJ PrePrints | http://dx.doi.org/10.7287/peerj.preprints.302v1 | CC-BY 3.0 Open Access | received: 25 Mar 2014, published: 25 Mar 2014

Table 3: Absolute redox potentials (V) of relevant redox pairs, computed at the B3LYP/6-311+G(d,p)// B3LYP/6-31G(d) level of theory. Solvation effects and corrections for pH=7.0 are included. "apoPChlide" and "apoChlide" refer to PChlide and Chlide devoid of Mg^{2+}. Despite ongoing controversy,(Donald et al., 2008) the absolute reaction potential of the standard hydrogen electrode in water is usually taken as 4.43 V.(Reiss & Heller, 1985)

	Redox half-reaction	ε =4	ε =10	ε =20	ε =78.36
a)	$NADPH^{2+} + 2\ e^- \rightarrow NADPH$	5.61	5.05	4.87	4.73
b)	C_{18}-Protonated PChlide + $2\ e^- + 1\ H^+ \rightarrow$ Chlide	5.36	5.29	5.27	5.25
c)	Fumaric acid + $2\ e^- + 2\ H^+ \rightarrow$ succinic acid	4.97	4.98	4.98	4.98
d)	PChlide + $2\ e^- + 2\ H^+ \rightarrow$ Chlide	4.93	4.94	4.94	4.94
e)	apoPChlide + $2\ e^- + 2\ H^+ \rightarrow$ apoChlide	4.53	4.53	4.53	4.53
f)	$NADP^+ + 2\ e^- + 1\ H^+ \rightarrow NADPH$	4.57	4.42	4.37	4.33
g)	PChlide + $2\ e^- + 1\ H^+ \rightarrow$ deprotonated Chlide	3.60	3.72	3.76	3.79
h)	$NADP^+ + 2\ e^- \rightarrow NADP^-$	3.02	3.01	3.00	3.00

The moderate barriers computed for the reaction mechanism raise an intriguing question: why does the light-dependent enzyme require an external driving force, as a quantum of light, to catalyze the reduction of the C_{17}=C_{18} bond in PChlide by NADPH? We have therefore compared the energies and redox potentials of several reaction intermediates to those of other biochemical redox models (Table 3). Direct comparison of the redox potential of NADPH (Table 3, line f) to that of the two-proton, two-electron conversion of PChlide to Chlide (Table 3, line d) shows that the PChlide reduction to Chlide by NADPH should be thermodynamically favored in the ground state. Further analysis of the the computed redox data shows that hydride transfer from NADPH (Table 3, line f) to PChlide to yield a *singly*-protonated, two-electron reduced PChlide (Table 3, line g) is thermodynamically disfavored, which entails that the spontaneity of the overall process arises from the addition of the second proton.

Furthermore, the energetic barrier for the direct hydride transfer in the ground state has previously been shown to be very high (>30 kcal.mol^{-1}(Heyes et al., 2009; Silva & Ramos, 2011)), even after accounting for quantum tunneling effects(Silva & Ramos, 2011). Ground-state hydride transfer from NADPH to the substrate therefore may only occur if it precedes the protonation event. Indeed, hydride transfer from NADPH to C_{18}-protonated PChlide (Figure 5) sould proceed efficiently with a negligible barrier (1.0 kcal mol^{-1}) and very high exergonicity (-33 kcal.mol^{-1}), but the actual feasibility of this step depends on the relative abundance of the C_{18}-protonated PChlide. Our computations on the dark-dependent PChOR, above, showed that the initial protonation of the C_{17}=C_{18} bond by carboxylic acids (the most acidic amino acid side chains present in proteins) is thermodynamically expensive by 20 kcal mol^{-1}, which means that the natural abundance of C_{18}-protonated PChlide is very small ($e^{-20 \text{ kcal mol/RT}}$). The overall barrier for the reduction of PChlide to Chlide by NADPH would therefore amount to at least those 20 kcal mol^{-1} + the 1.0 kcal.mol^{-1} barrier for the hydride trasnfer when the initial PChlide protonation is performed by a carboxylic acid (like Asp or Glu) and would be even larger when weaker acids are used (like the Tyr or Lys residues actually present in the light-dependent PChOR active site(Wilks & Timko, 1995)). Reduction of PChlide by NADPH therefore has too large an activation barrier to proceed at reasonable rates in the electronic ground state.

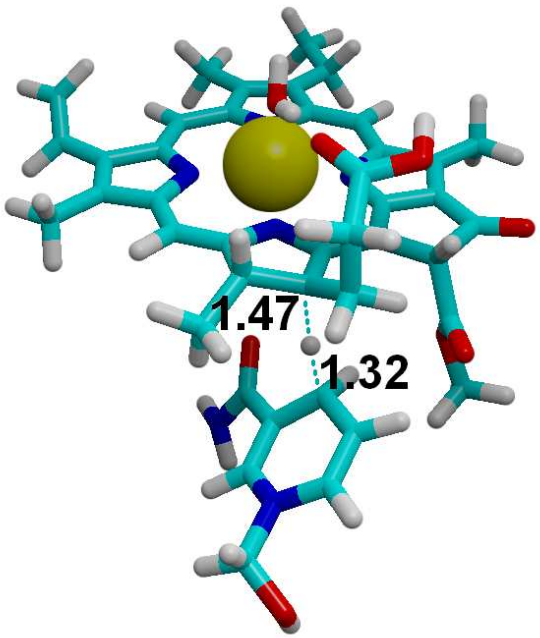

Figure 5: The transition state for the hydride transfer from NADPH to C_{18}-protonated PChlide. Highlighted distances in ångstrom.

More exotic pathways for ground-state reduction of PChlide by NADPH may also be excluded from consideration: for example, a two-electron transfer from NADPH to PChlide followed by energetically favorable H^+ transfer is also unfeasible, as the E° of the NADPH/$NADPH^{2+}$ pair (Table 3, line a) lies even farther above the PChlide substrate. On the other hand, two-electron transfer from a hypothetical (deprotonated) $NADP^-$ species (Table 3, line h), to PChlide (Table 3, line d), might be very favorable but is ruled out by the extreme difficulty of deprotonating NADPH: indeed, the difference of energies between NADPH and $NADP^-$ in water (337.2 $kcal.mol^{-1}$) is far higher than computed for even moderately weak acids (e.g. the difference between phenol and phenoxide(Silva, 2009) is only 299.2 $kcal.mol^{-1}$), which implies an extremely high pKa for the NADPH proton.

Tha preceding analysis explains the need for an external energetic event for the reduction of protochlorophyllide by NADPH. Incidentaly, our comparative analysis also showed that the two-electron/two-proton reduction of the double bond in PChlide, (Table 3, line d) is approximatley as favorable as the comparable reduction of the typical C-C double bond found in fumaric acid (Table 3, line c), whereas the absence of Mg^{2+} ion from PChlide disfavors this reduction process (Table 3, line e), which may explain why Mg^{2+} becomes inserted into the porphyrin ring before the reduction of the C_{17}=C_{18} bond.

Conclusions

We have analyzed the proton and electron transfer events in light-independent protochlorophyllide oxidoreductase. The reaction mechanism begins with single-electron reduction of the substrate by the

$(Cys)_3$Asp-ligated [4Fe-4S] yielding a negatively-charged intermediate which, depending on the rate of Fe-S cluster re-reduction, either receives two protons before the final reduction event or receives a proton from the propionic side chain present on ring D, is reduced by a second electron and then abstracts a proton from Asp274 in a barrier-less process. The energetic barrier of the second alternative lies well below the experimental values, which suggests that the rate-limiting step *in vivo* is most likely to reside in the ATP-dependent re-reduction(Kondo et al., 2011) of the $(Cys)_3$Asp-ligated [4Fe-4S] by the L-protein, or in the reduction of the L-protein by cytoplasmic electron donors, which we have not attempted to address.

This mechanism is made possible due to the low redox potential of the electron-donating $(Cys)_3$Asp-ligated 4Fe-4S cluster. In the light-dependent PChOR, this low-potential cluster is absent, and NADPH (which has a higher redox potential) is used as the electron donor. All possibilities of electron/hydride transfer from NADPH to PChlide were shown by our computations to be highly disfavored, clearly showing the reason behind the requirement for a quantum of light in the NADPH-dependent protochlorophyllide oxidoreductase, as it provides the energy needed to overcome this thermodynamically disfavored process by generating a more easily reducible state of the PChlide substrate.(Silva & Ramos, 2011)

Supporting Information: Geometries and energies of every molecule described.

References

Baker, J., Kessi, A., & Delley, B. 1996. *The generation and use of delocalized internal coordinates in geometry optimization*. Journal of Chemical Physics 105:192–212.

Becke, A. D. 1993. *Density-functional thermochemistry. III. The role of exact exchange*. The Journal of Chemical Physics 98(7):5648–5652.

Blomberg, M. R. A., & Siegbahn, P. E. M. 2003. *A quantum chemical study of tyrosyl reduction and O—O bond formation in photosystem II*. Molecular Physics 101(1-2):323–333.

PeerJ PrePrints | http://dx.doi.org/10.7287/peerj.preprints.302v1 | CC-BY 3.0 Open Access | received: 25 Mar 2014, published: 25 Mar 2014

Bröcker, M. J., Schomburg, S., Heinz, D. W., Jahn, D., Schubert, W., & Moser, J. 2010. *Crystal structure of the nitrogenase-like dark operative protochlorophyllide oxidoreductase catalytic complex (ChlN/ChlB)2.* The Journal of biological chemistry 285(35):27336–45.

Cossi, M., Mennucci, B., Pitarch, J., & Tomasi, J. 1998. *Correction of cavity-induced errors in polarization charges of continuum solvation models*. Journal of Computational Chemistry 19(8):833–846.

Donald, W. A., Leib, R. D., O'Brien, J. T., Bush, M. F., & Williams, E. R. 2008. *Absolute standard hydrogen electrode potential measured by reduction of aqueous nanodrops in the gas phase.* Journal of the American Chemical Society 130(11):3371–3381.

Fujita, Y., & Bauer, C. E. 2000. *Reconstitution of light-independent protochlorophyllide reductase from purified bchl and BchN-BchB subunits. In vitro confirmation of nitrogenase-like features of a bacteriochlorophyll biosynthesis enzyme.* The Journal of biological chemistry 275(31):23583–8.

Fujita, Y., & Bauer, C. E. 2003. *A Nitrogenase-Like Enzyme Catalyzing a Key Reaction for Greening in the Dark*. In K. M. Kadish, K. M. Smith, & R. Guilard (Eds.), The Porphyrin Handbook: Chlorophylls And Bilins: Biosynthesis, Synthesis And Degradation (Vol. 13, pp. 109–156). Academic Press.

Granovsky, A. A. 2013. *Firefly 8.0.0*.

Greco, C., Fantucci, P., Ryde, U., & Gioia, L. de. 2010. *Fast generation of broken-symmetry states in a large system including multiple iron-sulfur assemblies: Investigation of QM/MM energies, clusters charges, and spin populations*. International Journal of Quantum Chemistry 111(2011):39493960.

Grimme, S., Antony, J., Ehrlich, S., & Krieg, H. 2010. *A consistent and accurate ab initio parametrization of density functional dispersion correction (DFT-D) for the 94 elements H-Pu.* The Journal of chemical physics 132(15):154104.

Hertwig, R. H., & Koch, W. 1995. *On the accuracy of density functionals and their basis set dependence: An extensive study on the main group homonuclear diatomic molecules Li2 to Br2*. Journal of Computational Chemistry 16(5):576–585.

Heyes, D. J., & Hunter, C. N. 2004. *Identification and characterization of the product release steps within the catalytic cycle of protochlorophyllide oxidoreductase.* Biochemistry 43(25):8265–71.

Heyes, D. J., Levy, C., Sakuma, M., Robertson, D. L., & Scrutton, N. S. 2011. *A twin-track approach has optimized proton and hydride transfer by dynamically coupled tunneling during the evolution of protochlorophyllide oxidoreductase.* The Journal of biological chemistry 286(13):11849–54.

Heyes, D. J., Sakuma, M., de Visser, S. P., & Scrutton, N. S. 2009. *Nuclear quantum tunneling in the light-activated enzyme protochlorophyllide oxidoreductase.* The Journal of biological chemistry 284(6):3762–7.

Kelly, C. P., Cramer, C. J., & Truhlar, D. G. 2006. *Aqueous solvation free energies of ions and ion-water clusters based on an accurate value for the absolute aqueous solvation free energy of the proton*. Journal of Physical Chemistry B 110:16066–16081.

Kondo, T., Nomata, J., Fujita, Y., & Itoh, S. 2011. *EPR study of 1Asp-3Cys ligated 4Fe-4S iron-sulfur cluster in NB-protein (BchN-BchB) of a dark-operative protochlorophyllide reductase complex.* FEBS letters 585(1):214–8.

Lee, C., Yang, W., & Parr, R. G. 1988. *Development of the Colle-Salvetti correlation-energy formula into a functional of the electron density*. Physical Review B 37(2):785–789.

Masuda, T., & Fujita, Y. 2008. *Regulation and evolution of chlorophyll metabolism.* Photochemical & photobiological sciences : Official journal of the European Photochemistry Association and the European Society for Photobiology 7(10):1131–1149.

Masuda, T., & Takamiya, K.-I. 2004. *Novel Insights into the Enzymology, Regulation and Physiological Functions of Light-dependent Protochlorophyllide Oxidoreductase in Angiosperms.* Photosynthesis research 81(1):1–29.

Mennucci, B., & Tomasi, J. 1997. *Continuum solvation models: A new approach to the problem of solute's charge distribution and cavity boundaries*. Journal of Chemical Physics 106(12):5151–5158.

Moss, G. P. 1987. *Nomenclature of tetrapyrroles*. Pure Appl. Chem 59:779–832.

Muraki, N., Nomata, J., Ebata, K., Mizoguchi, T., Shiba, T., Tamiaki, H., Kurisu, G., & Fujita, Y. 2010. *X-ray crystal structure of the light-independent protochlorophyllide reductase.* Nature 465(7294):110–114.

Niu, S., & Ichiye, T. 2009. *Insight into environmental effects on bonding and redox properties of [4Fe-4S] clusters in proteins.* Journal of the American Chemical Society 131(16):5724–5.

Reiss, H., & Heller, A. 1985. *The absolute potential of the standard hydrogen electrode: a new estimate*. The Journal of Physical Chemistry 89(20):4207–4213.

Sarma, R., Barney, B. M., Hamilton, T. L., Jones, A., Seefeldt, L. C., & Peters, J. W. 2008. *Crystal structure of the L protein of Rhodobacter sphaeroides light-independent protochlorophyllide reductase with MgADP bound: a homologue of the nitrogenase Fe protein.* Biochemistry 47(49):13004–15.

Schmidt, M. W., Baldridge, K. K., Boatz, J. A., Elbert, S. T., Gordon, M. S., Jensen, J. H., Koseki, S., Matsunaga, N., Nguyen, K. A., Su, S., et al. 1993. *General atomic and molecular electronic structure system*. Journal of Computational Chemistry 14(11):1347–1363.

Silva, P. J. 2009. *Inductive and resonance effects on the acidities of phenol, enols, and carbonyl alpha-hydrogens.* The Journal of organic chemistry 74(2):914–6.

Silva, P. J., & Ramos, M. J. 2011. *Computational insights into the photochemical step of the reaction catalyzed by protochlorophylide oxidoreductase*. International Journal of Quantum Chemistry 111(7-8):1472–1479.

Swart, M., Güell, M., Luis, J. M., & Solà, M. 2010. *Spin-state-corrected Gaussian-type orbital basis sets.* The Journal of Physical Chemistry A 114(26):7191–7197.

Sytina, O. A., van Stokkum, I. H. M., Heyes, D. J., Hunter, C. N., & Groot, M. L. 2012. *Spectroscopic characterization of the first ultrafast catalytic intermediate in protochlorophyllide oxidoreductase.* Physical chemistry chemical physics 14(2):616–625.

Szilagyi, R. K., & Winslow, M. A. 2006. *On the accuracy of density functional theory for iron—sulfur clusters*. Journal of Computational Chemistry 27(12):1385–1397.

Takano, Y., Yonezawa, Y., Fujita, Y., Kurisu, G., & Nakamura, H. 2011. *Electronic structures of a [4Fe–4S] cluster, [Fe4S4(SCH3)3(CH3COO)], in dark-operative protochlorophyllide oxidoreductase (DPOR)*. Chemical Physics Letters 503(4-6):296–300.

Tissandier, M. D., Cowen, K. A., Feng, W. Y., Gundlach, E., Cohen, M. H., Earhart, A. D., Coe, J. V, & Tuttle, T. R. 1998. *The Proton's Absolute Aqueous Enthalpy and Gibbs Free Energy of Solvation from Cluster-Ion Solvation Data*. The Journal of Physical Chemistry A 102(40):7787–7794.

Tomasi, J., & Persico, M. 1994. *Molecular Interactions in Solution: An Overview of Methods Based on Continuous Distributions of the Solvent*. Chemical Reviews 94(7):2027–2094.

Wilks, H. M., & Timko, M. P. 1995. *A Light-Dependent Complementation System for Analysis of NADPH: Protochlorophyllide Oxidoreductase: Identification and Mutagenesis of Two Conserved Residues that are Essential for Enzyme Activity*. Proceedings of the National Academy of Sciences 92(3):724–728.